IOP Publishing | Institute of Physics and Engineering in Medicine Physiological Measurement

Physiol. Meas. **38** (2017) 1405–1425 https://doi.org/10.1088/1361-6579/aa7652

Atrial fibrillation detection on compressed sensed ECG

Giulia Da Poian[1,2], Chengyu Liu[1], Riccardo Bernardini[2], Roberto Rinaldo[2] and Gari D Clifford[1,3]

[1] Department of Biomedical Informatics, Emory University, Atlanta, GA, United States of America
[2] Dipartimento Politecnico di Ingegneria e Architettura, University of Udine, Udine, Italy
[3] Department of Biomedical Engineering, Georgia Institute of Technology, Atlanta, GA, United States of America

E-mail: dapoian.giulia@spes.uniud.it

Received 27 March 2017, revised 22 May 2017
Accepted for publication 1 June 2017
Published 27 June 2017

Abstract

Objective: Compressive sensing (CS) approaches to electrocardiogram (ECG) analysis provide efficient methods for real time encoding of cardiac activity. In doing so, it is important to assess the downstream effect of the compression on any signal processing and classification algorithms. CS is particularly suitable for low power wearable devices, thanks to its low-complex digital or hardware implementation that directly acquires a compressed version of the signal through random projections. In this work, we evaluate the impact of CS compression on atrial fibrillation (AF) detection accuracy. *Approach*: We compare schemes with data reconstruction based on wavelet and Gaussian models, followed by a P&T-based identification of beat-to-beat (RR) intervals on the MIT-BIH atrial fibrillation database. A state-of-the-art AF detector is applied to the RR time series and the accuracy of the AF detector is then evaluated under different levels of compression. We also consider a new beat detection procedure which operates directly in the compressed domain, avoiding costly signal reconstruction procedures. *Main results*: We demonstrate that for compression ratios up to 30% the AF detector applied to RR intervals derived from the compressed signal exhibits results comparable to those achieved when employing a standard QRS detector on the raw uncompressed signals, and exhibits only a 2% accuracy drop at a compression ratio of 60%. We also show that the Gaussian-based reconstruction approach is superior in terms of AF detection accuracy, with a negligible drop in performance at a compression ratio $\leqslant$75%, compared to a wavelet approach, which exhibited a significant drop in accuracy at a compression ratio $\geqslant$65%. *Significance*: The

results suggest that CS should be considered as a plausible methodology for both efficient real time ECG compression (at moderate compression rates) and for offline analysis (at high compression rates).

Keywords: atrial fibrillation, compressive sensing, ECG

(Some figures may appear in colour only in the online journal)

1. Introduction

Atrial fibrillation (AF) is the most common super-ventricular arrhythmia and consists of an abnormal electrical activity arising in the atrium (Camm *et al* 2010). Although it is not a lethal disease, it may lead to very disabling complications such as cardiac failure and atrial thrombosis, with the subsequent risk of a stroke (Lip *et al* 2016). In order to diagnose the arrhythmia, it is important to document the heart rhythm at the time of symptoms (e.g. palpitations, syncope, chest pain) with electrocardiography. In presence of AF, the electrocardiogram (ECG) is characterized by absent P-waves and irregularity of the ventricular response. The AF patient exhibits irregular rhythms at rates between 100 and 175 beats per minute, while a normal sinus rhythm has a resting heart rate between 60 and 100 beats per minute.

If a suspected arrhythmia cannot be detected and documented on a resting ECG during medical examination, the cardiac rhythm may be recorded for 24 or 48 h using portable Holter monitoring devices. Despite the undeniable benefits of such medium term ECG monitoring, some arrhythmias might not be detected (because they are too infrequent or asymptomatic/'silent'). The extension of ECG recording to 7 d or more, using wearable or implantable devices, can be necessary to detect critical episodes.

Wireless body sensor networks allow new scenarios for providing continuous monitoring of physiological signals using wearable devices (Alemdar and Ersoy 2010, Ko *et al* 2010). In particular, this technology enables long-term/real-time monitoring without restricting the person's regular activities and reducing hospitalization costs. As data storage and transmission are major power consumers in embedded devices, data compression will result in improved transmission efficiency, reduced storage requirements, lower power consumption and longer battery life.

Lately, compressive sensing (CS) has demonstrated promising results for this scenario (Candès *et al* 2006a, Donoho 2006, Baraniuk 2007). CS is capable to achieve high compression ratios with low computational and memory requirements, making it suitable for use in embedded nodes of a wireless body sensor network (Mamaghanian *et al* 2011). CS theory states that signals which are sparse in some domain, i.e. which can be represented by few coefficients, can be fully reconstructed using only a small number of linear measurements, taken at a rate that is much smaller than that required by Nyquist-rate sampling. When dealing with real-world ECG signals, the sparsity requirement is in general not fulfilled exactly. However, the reconstruction process enables the recovery of an approximation of the original signal from compressed measurements. In the reconstruction of physiological signals, it is essential to guarantee that all clinically relevant information for a given task is preserved, in order to prevent significant degradation in the performance of any standard (or novel) algorithm.

In this paper, we investigate the impact of CS on AF detection. After CS signal reconstruction, the 'Pan and Tompkins' (P&T) R-peak (or 'QRS complex') detection algorithm (Pan and Tompkins 1985) is applied, and the resulting RR interval series is analyzed to identify AF episodes. The reconstruction process might introduce distortion leading to inaccurate R-peak detection and

consequently to a degradation in the ability to identify AF. The aim of this work is to quantify the performance of an AF detection algorithm on reconstructed signals at different compression ratios.

Since the recovery process involves algorithms with a relatively high computational load, recovering the entire long term recording might require long time and considerable resources. Thus, we also evaluate the reliability of a QRS detector that works directly on the compressed measurements. Using this, it is possible to perform the AF detection without recovering the original ECG signal. For this scenario, we also assess the performance of the AF detector at different compression ratios.

The remainder of this paper is organized as follows. In section 2, we provide an overview of the experiments that we carry out in order to assess the effect of different compression ratios and reconstruction/detection methods on AF detection. Data from the MIT atrial fibrillation dataset (Tateno and Glass 2000) were used for reference. We also present a brief review of the CS paradigm, of heart beat detection on compressed measurements and of an AF detection method based on multi-feature extraction and a support vector machine (SVM). The evaluation metrics are also described in this section. Then, a series of experimental results are presented in section 3 and discussed in section 4. Finally, in section 5 we conclude this study.

2. Method

2.1. Method description

The work-flow adopted for the AF evaluation process is reported in figure 1. It clarifies the AF evaluation procedure to assess the effect of different CS compression ratios on AF detection.

First, we consider the uncompressed scenario, i.e. AF detection based on the QRS annotations directly available in the MIT atrial fibrillation database (MIT AF DB) (Tateno and Glass 2000), as well as AF detection based on the detected QRS locations from the uncompressed aw ECG signals using the P&T detection algorithm (Pan and Tompkins 1985). An AF detection method based on multi-feature extraction and the SVM detector, described in section 2.6, is applied to the RR interval series to perform AF detection.

For the assessment of AF accuracy on compressed ECG signals, we consider three different scenarios, in addition to different values of compression ratios. The first two scenarios require the reconstruction of the ECG signals from compressed measurements as explained in section 2.4, where two different sparsifying bases are adopted. Then, R-peak detection is performed using the P&T algorithm on the reconstructed signals. The third scenario evaluated in this study is motivated by the desire to simplify the detection process after compression. In particular, this scenario does not require signal reconstruction and the R-peaks are directly detected using an algorithm that operates on the compressed ECG signals. The detector, based on matched filtering, is described in section 2.5, and is herein referred to as compressed sensing matched filtering (CSMF). After extraction of the RR interval time series, the multi-feature SVM detector is also applied for AF detection.

Finally, in order to verify that clinically relevant information is preserved, AF detection accuracy is assessed in a range of compression ratios, i.e. 10, 20, 30, 40, 50, 60, 65, 70, 75, 80, 85 and 90%. In addition, we also evaluated the accuracy of QRS detection in the three different scenarios. In this way, we can verify the relation between a good R-peak detection and the ability of correctly classify an AF episode.

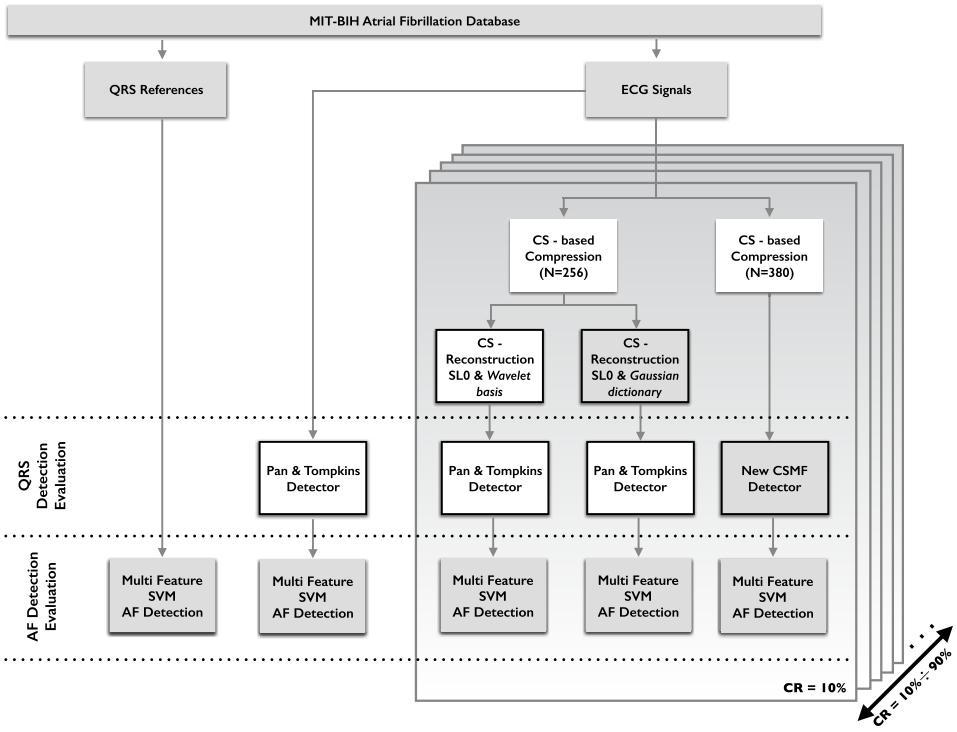

Figure 1. General flowchart of the evaluation method employed in this work.

2.2. Data

For the analysis in this article, ECG signals from the MIT atrial fibrillation dataset (Tateno and Glass 2000), freely accessible on PhysioNet (Goldberger *et al* 2000), are used. This database contains 25 ECG recordings with a duration of approximately 10 h each, sampled at 250 Hz, 12 bit resolution, with accompanying expert beat annotations. Among the records, 23 records include raw two-channel ECG signals and only the first one of each recording is used in this study. For two recordings, i.e. records 00735 and 03665, the ECG signal is missing and represented only by the rhythm and QRS beat annotation files. They are therefore excluded by this study since it is not possible to apply the proposed method without the raw ECG signals. For each signal, QRS annotations, derived using an automated detector, are provided along with rhythm information manually annotated by experts. Four rhythm types are reported: AF (atrial fibrillation), AFL (atrial flutter), J (AV junctional rhythm), and N (used to indicate all other rhythms). In particular, this database includes 21 recordings with paroxysmal AF (episodes of AF for each subject varies from 2 to 39) and two recordings in persistent AF. Data profiles were detailed in table 1. The RR interval series corresponding to the latter three rhythm types (AFL, J and N) were merged as non-AF rhythms in this study, to create AF and non-AF rhythm types.

2.3. A compressive sensing overview

CS is a relatively new signal processing framework that enables the acquisition of a compressed version of sparse or compressible signals (Candès *et al* 2006a, Donoho 2006, Baraniuk 2007).

Table 1. Profile of MIT-BIH AF database separated by the four different rhythm types.

		Non-AF rhythm			
Variable	AF rhythm	N	AFL	J	Total
Total no. of rhythm episodes	299 (48.0%)	292 (46.9%)	14 (2.2%)	18 (2.9%)	324 (52.0%)
Total no. of QRS annotations	521 415 (42.6%)	663 202 (54.2%)	117 10 (1.0%)	268 18 (2.2%)	701 730 (57.4%)
Total time length (hour)	93.5 (37.5%)	149.1 (59.8%)	1.4 (0.6%)	5.2 (2.1%)	155.7 (62.5%)
Min no. of QRS in each episode	3	5	9	2	—
Mean no. of QRS in each episode	1744	2271	836	1490	—
Max no. of QRS in each episode	618 91	368 34	6322	263 65	—
Min time in each episode (h)	0.0005	0.0012	0.0010	0.0004	—
Mean time in each episode (h)	0.31	0.51	0.10	0.29	—
Max time in each episode (h)	10.2	8.9	0.7	5.1	—

The process is attractive for low complexity compression solutions, and in particular for low power sensing devices. In fact, it turns out that, since it simply calculates random compressive measurements, the sensor encoder does not require any particular assumption about the signal, besides sparsity, and is therefore universal. Moreover, measurements can be computed very efficiently by means of digital or analog schemes.

An N-dimensional signal vector is k- *sparse* if it has only $k < N$ non-zero components. CS theory shows that it is possible to reconstruct a sparse signal $\mathbf{x} \in \mathbb{R}^N$ from a small number of random projections

$$\mathbf{y} = \mathbf{\Phi}\mathbf{x}, \tag{1}$$

where $\mathbf{y} \in \mathcal{R}^M$, $M \sim k < N$, is the vector containing the compressed measurements, and $\mathbf{\Phi} \in \mathcal{R}^{M \times N}$ is the projection matrix, usually called the *sensing* matrix.

In real world applications, we deal with nearly sparse signals and measurement noise, and the problem in equation (1) becomes

$$\mathbf{y} = \mathbf{\Phi}\mathbf{x} + \mathbf{n}, \tag{2}$$

where $\mathbf{n}$ is an additive term taking error into account.

The reconstruction of $\mathbf{x}$ from $\mathbf{y}$ is in general an ill-posed problem, since the system in equation (2) is underdetermined. Moreover, note that a non-sparse signal $\mathbf{x}$ can be typically written as

$$\mathbf{x} = \mathbf{\Psi}\mathbf{s}, \tag{3}$$

with $\mathbf{s}$ sparse. In equation (3), $\mathbf{\Psi}$ may be a basis matrix, $\mathbf{\Psi} \in \mathcal{R}^{N\times N}$, or an over-complete dictionary, $\mathbf{\Psi} \in \mathcal{R}^{P\times N}$. In this last case, the dimension P is higher than that of $\mathbf{x}$. By assuming sparsity of the signal and some properties for matrix $\mathbf{\Phi}$ (or $\mathbf{\Phi\Psi}$ in the more general case), reconstruction is possible.

In particular, to recover the signal from the measurements, one can intuitively search for the sparsest solution, i.e. the one with smallest support, and solve the following minimization problem

$$\arg\min_{s} \|\mathbf{s}\|_0 \text{ subject to } \|\mathbf{y} - \mathbf{\Phi\Psi}\mathbf{s}\|_2 \leqslant \epsilon, \tag{4}$$

where $\|\cdot\|_0$ denotes the l_0 pseudo-norm counting the number of non-zero elements in vector $\mathbf{s}$ and ϵ is a bound on the noise energy, i.e. $\|\mathbf{n}\|_2 \leqslant \epsilon$. The original signal $\mathbf{x}$ can be finally recovered thanks to the relation in equation (3).

The properties that a sensing matrix should have in order to guarantee perfect recovery have been carefully addressed in the literature. We mention here the restricted isometry property (RIP) (Candès 2008), which requires that any two distinct sparse vectors in the original space are mapped to the compressed domain approximately preserving their distance. The RIP ensures that a variety of practical algorithms guarantee near-optimal recovery of any sparse/compressible signal. Several methods have been proposed in order to solve the problem in equation (4) by convex relaxation, such as basis pursuit denoising (BPDN), where l_0 is replaced by the l_1 norm to make the problem tractable

$$\arg\min_{s} \|\mathbf{s}\|_1 \text{ subject to } \|\mathbf{y} - \mathbf{\Phi\Psi}\mathbf{s}\|_2 \leqslant \epsilon, \tag{5}$$

and by greedy algorithms such as matching pursuit and orthogonal matching pursuit. Another approach is to solve the recovery problem by replacing the l_0 norm with a smooth approximation of it. The resulting smoothed l_0 norm (SL0) (Mohimani *et al* 2009) algorithm has a better performance than the greedy algorithms while requiring considerably less computation time than state-of-the-art l_1 minimization solvers.

2.4. Setting the CS parameters

In our work, when signal compression is followed by reconstruction, CS is applied to non-overlapping windows (blocks) of length $N = 256$ samples, which corresponds to almost one second in the MIT AF DB ECG data. We chose N equal to a power of two to allow the use of a dyadic wavelet matrix $\mathbf{\Psi}$ as the sparsifying basis, as described below. Moreover, using windows corresponding to approximately one second, makes the compression process suitable for low-delay real-time applications.

Each signal is compressed using a different random sensing matrix with i.i.d. entries drawn from the normal distribution, $\mathbf{\Phi}_{i,j},\ j \in \mathcal{N}(0, 1/M)$. In a realistic implementation the resulting measurements $\mathbf{y},\ y_j = \sum_{i=1}^{N} \phi_{ji} x_i$ must be represented with a finite number of bits. In this work we use a uniform scalar quantizer with $B = 12$-bit of resolution, having $L = 2^{12}$ quantization levels with equal width $\Delta = r2^{-B}$, where r is the dynamic range of the measurements. Each value y_i is rounded to the nearest multiple of Δ.

Signal reconstruction from CS measurements is performed using the SL0 algorithm (Mohimani *et al* 2009). Since the reconstruction process is based on the signal sparsity assumption, we need to use a sparsifying transform $\mathbf{\Psi}$. To this end, we employ the orthogonal Daubechies-4 wavelets (Db4), and a 5-level decomposition, which can effectively provide a sparse representations of the ECG, as suggested in Pinheiro *et al* (2010a).

We also compare the wavelet basis to the use of an over-complete Gaussian dictionary introduced in Da Poian *et al* (2014), which provides a sparse representation of ECG signals. Since it is based on the ECG morphology, it preserves the shape of QRS complexes as well as of P and T waves, increasing the quality of reconstructed signals.

In this study we also verify the performance of a beat detector that operates directly on the compressed sensed measurements and does not require signal reconstruction. In particular we use CSMF, a newly introduced QRS detection technique described in section 2.5. For this method, it is required that the signal block contains at least one heart beat in the majority of cases, so we set $N = 380$, corresponding to about 1.5 s block duration. The sensing matrices are still drawn from an i.i.d. standard normal distribution, $\mathbf{\Phi}_{i,j}, j \in \mathcal{N}(0, 1/M)$.

2.5. CSMF-based QRS detection

Some signal processing problems do not require full signal reconstruction, and it is indeed possible to directly process compressive measurements and extract information. Recently, we proposed a new beat detector that works on compressed measurements (Da Poian *et al* 2017). It is based on template matching, or matched filtering, which has been used extensively in the uncompressed domain (see, for example, Hamilton and Tompkins (1986), Kaplan (1990) and Ruha *et al* (1997).) It calculates a template in the compressed domain (the compressed average QRS complex), and estimates the correlation between the compressed ECG signal and the compressed template.

Specifically, the procedure consists of three main steps, namely, (1) QRS template construction, (2) correlation estimation using matched filtering on compressive measurements and (3) peak-finding based on adaptive thresholding in the correlation time series.

First, a short uncompressed or reconstructed signal segment is used to identify the QRS complexes and to generate the template. This ECG segment should be sufficiently long to ensure that it contains enough beats (e.g. 10 s). The P&T detector is then used to detect the beats and form the template ψ in the signal domain, before being mapped to the compressed domain.

It is possible to show that given the template ψ, the sensing matrix $\mathbf{\Phi}$ and the measurements $\mathbf{y}$, the cross-correlation coefficients $R_{x\psi}(n) = \sum_\tau x_r(\tau)\psi(\tau - n)$, can be effectively estimated, under appropriate hypotheses, by

$$\hat{\mathbf{R}}_{\mathbf{x}\psi,n} = \frac{N}{M}\langle \mathbf{y}, (\mathbf{\Phi}\mathbf{\Phi}^T)^{-1}\mathbf{\Phi}\psi_n\rangle, \tag{6}$$

where $\mathbf{\Phi}\psi_n$ is the *compressed* template (after translation around the current sample n). In other words, the inner product corresponding to the calculation of $R_{x\psi}(n)$, for each n, can be approximated by the inner product (6) in the compressed domain.

The third and final stage implements QRS detection by comparing the absolute value of the correlation against an adaptive amplitude-dependent threshold, which depends on the root mean square (RMS) value of the cross-correlation in the current window (corresponding to 1.5 s). After the RMS value is calculated, if it is larger than 25% of the maximum

cross-correlation absolute value, the threshold is set to be 75% of the maximum value of the segment. If the RMS of the segment is less than 25% of its maximum value, the threshold is set to be 50% of the maximum value. The procedure is not very sensitive to small changes in these threshold values, which were derived by experiments. To avoid false detection, a refractory period (in which QRS detection is prohibited) of 200 ms is employed prior to repeating the process for the next cardiac cycle. Additionally, decision rules for the reduction of false positives are applied, to avoid detection of QRS complexes located in between two consecutive blocks. In particular, when the time between the last detected peak in the previous block and the first detected beat in the current block is less then 200 ms, the middle point is taken as the R-peak location. Similarly, missed beats can occur between two consecutive blocks. In order to deal with this, when the RR interval measured across two blocks is greater than 1.5 times the average RR interval computed on the previous 10 signal blocks, the threshold is adjusted to the half of its value and a new search is performed on a window of 100 ms centered between the two blocks.

2.6. AF detection using SVM

Generally, AF detectors are based on two approaches. One is based on atrial activity analysis and it focuses on the absence of P waves in the ECG signal. However, the P-wave has relatively low amplitude, and the ambulatory ECG often exhibits movement-related noise resembling the P-wave, which can lead to many false positives. The second approach is based on ventricular response analysis, and it is based on the predictability of the beat-to-beat intervals of the ventricular contractions. These RR intervals are derived from the most obvious large amplitude feature in the ECG, the R-peak. This approach is robust to artifacts, and is suitable for analysis of ECG recorded by wearable devices (Carrara *et al* 2015).

In this study, we used a state-of-the-art method developed in our earlier work for the ventricular response-based AF detection (Li *et al* 2016), which was developed on the MIT AF DB described in section 2.2. The AF classification step is based on a SVM applied to 8 features that quantify irregularity in the RR interval time series. The SVM is trained by considering 30 s long signal windows, manually marked as AF and non-AF rhythms (Li *et al* 2016).

2.7. Evaluation metrics

2.7.1. Compression. The compression ratio (CR) parameter takes into account the number of bits necessary to represent each sample both in the CS and original signal domains. Since in this work we use the same number of quantization bits in both domains, CR is computed as

$$\mathrm{CR} = \frac{N - M}{N}, \tag{7}$$

where M represents the number of samples in the CS domain and N is the number of samples in the original signal.

2.7.2. Evaluation of QRS detection accuracy. A QRS is correctly identified if the time difference between the annotated QRS in the reference and the detected R-peak is smaller than or equal to 50 ms, according to the recommendation of the American national standard for ambulatory ECG analyzers (ANSI/AAMI EC38-1994) (Association for the Advancement of

Medical Instrumentation 1994). We compute the sensitivity ($\mathrm{Se_{QRS}}$) and positive predictivity ($+\mathrm{P_{QRS}}$) for QRS detection as

$$\mathrm{Se_{QRS}} = \frac{\mathrm{TP_{QRS}}}{\mathrm{TP_{QRS}} + \mathrm{FN_{QRS}}},$$
$$+\mathrm{P_{QRS}} = \frac{\mathrm{TP_{QRS}}}{\mathrm{TP_{QRS}} + \mathrm{FP_{QRS}}},$$

where $\mathrm{TP_{QRS}}$ (true positives) is the number of QRS complexes correctly located by the detector, $\mathrm{FN_{QRS}}$ (false negative) is the number of missing true beats and $\mathrm{FP_{QRS}}$ (false positive) represents the number of false beat detections.

Accurate R-peak detection is crucial for a reliable analysis of AF episodes. In order to test QRS detection accuracy, record 07126 was excluded since its reference QRS annotations are not consistent with the ECG signal.

2.7.3. Evaluation of AF detection accuracy. For this purpose, the RR series are classified into AF episodes and non-AF episodes. The classification is performed with the detector of section 2.6, on the basis of 30 consecutive detected beat positions. In particular, the manually annotated AF and non-AF time intervals are divided into segments of 30 consecutive beats, possibly discarding the last segment if it contains less then 30 beats, and each of these segments is classified by the detector.

The accuracy of AF classification adopted in this work use the following metrics

$$\text{Sensitivity}: \ \mathrm{Se} = \frac{TP}{TP + FN},$$
$$\text{Specificity}: \ \mathrm{Sp} = \frac{TN}{TN + FP},$$
$$\text{Accuracy}: \ \mathrm{Acc} = \frac{TP + TN}{TP + FP + TN + FN},$$
$$\text{Positive predictivity value}: \ \mathrm{PPV} = \frac{TP}{TP + FP},$$
$$\text{Negative predictivity value}: \ \mathrm{NPV} = \frac{TN}{TN + FN},$$
$$\text{Youden index}: \ J = \mathrm{Se} + \mathrm{Sp} - 1,$$

where *TP*, *FN*, *FP* and *TN* denote the true positive, false negative, false positive and true negative detections, respectively. All the measures were computed on all the RR interval series within the dataset, including noisy segments to represent a real world scenario.

3. Results

3.1. QRS detection performance

Figures 2(a)–(c) show $\mathrm{TP_{QRS}}$, $\mathrm{FN_{QRS}}$ and $\mathrm{FP_{QRS}}$ for QRS detection using the considered three approaches, namely the CSMF R-peak detector in the compressed domain, the P&T detector after signal reconstruction using the wavelet basis (WT) and the Gaussian dictionary (GD). Figure 2(d) shows the total number of detected QRS, i.e. the sum of $\mathrm{TP_{QRS}}$ and $\mathrm{FP_{QRS}}$ as a function of the compression ratio.

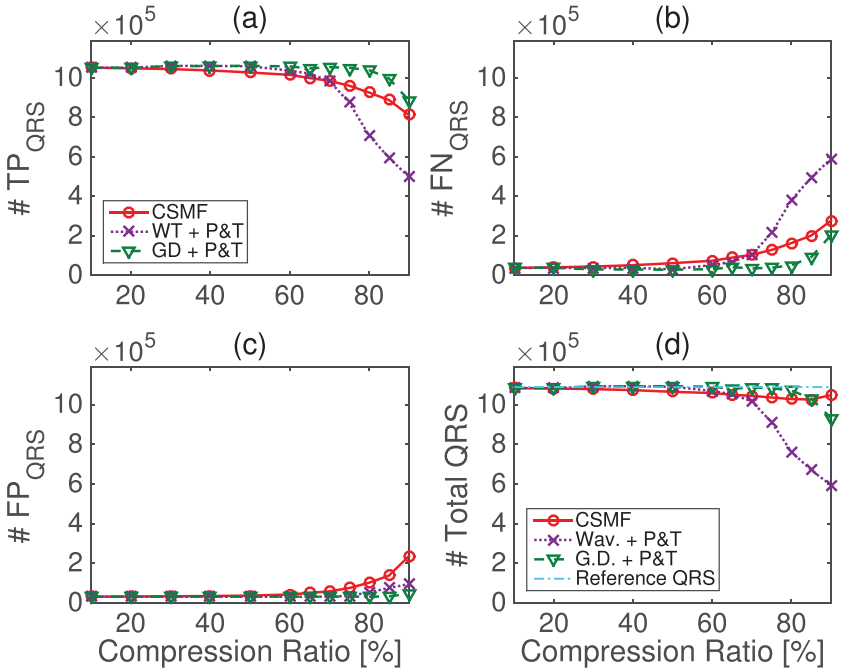

Figure 2. Numbers of (a) TP_{QRS}, (b) FN_{QRS} and (c) FP_{QRS}. (d) Total number of the detected QRS (TP_{QRS}+FP_{QRS}) varying the compression ratio for the CSMF detection or Pan and Tompkins (P&T) detection after reconstruction using wavelet transform (WT) and Gaussian dictionary (GD).

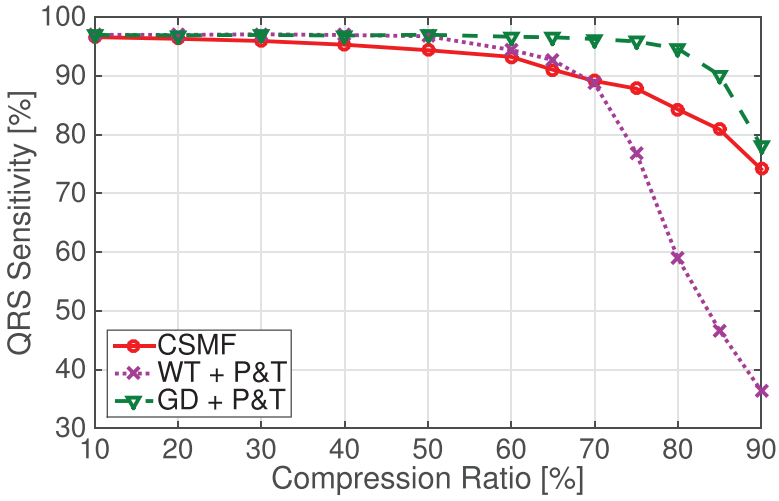

Figure 3. QRS detection sensitivity versus CR.

As a reference for the performance of detection in compressed/reconstructed signals, we applied the P&T QRS detector (Pan and Tompkins 1985) on the raw original ECG signals, obtaining $Se_{QRS} = 96.38\%$, $+P_{QRS} = 90.38\%$.

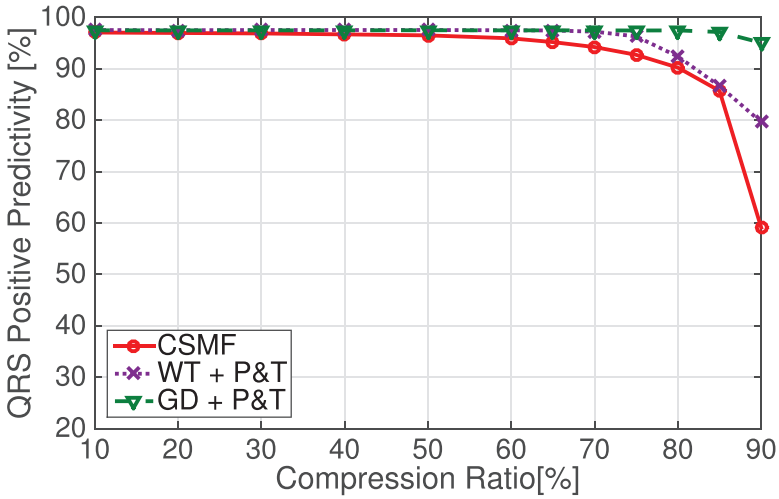

Figure 4. QRS detection positive predictivity versus CR.

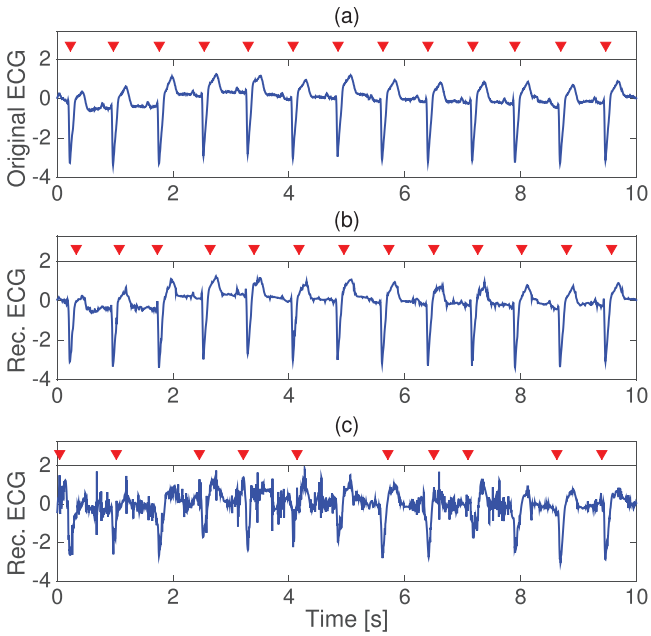

Figure 5. (a) Original ECG signal (first 10 s of record 05121) and reference QRS annotations. (b) Signal recovered at 75% compression using Gaussian dictionary and QRS positions detected using the P&T algorithm. (c) Signal recovered at 75% compression using wavelet transform (WT) and QRS positions detected using the P&T algorithm.

Figures 3 and 4 illustrate the results of QRS detection sensitivity (Se_{QRS}) and positive predictivity ($+P_{QRS}$) as a function of the compression ratio. At low CR levels (CR $< 60\%$), QRS detection using the three CS approaches gives similar results. For CR $= 10\%$, the CSMF method results are $Se_{QRS} = 96.61\%$ and $+P_{QRS} = 97.06\%$. The P&T method run on the reconstructed

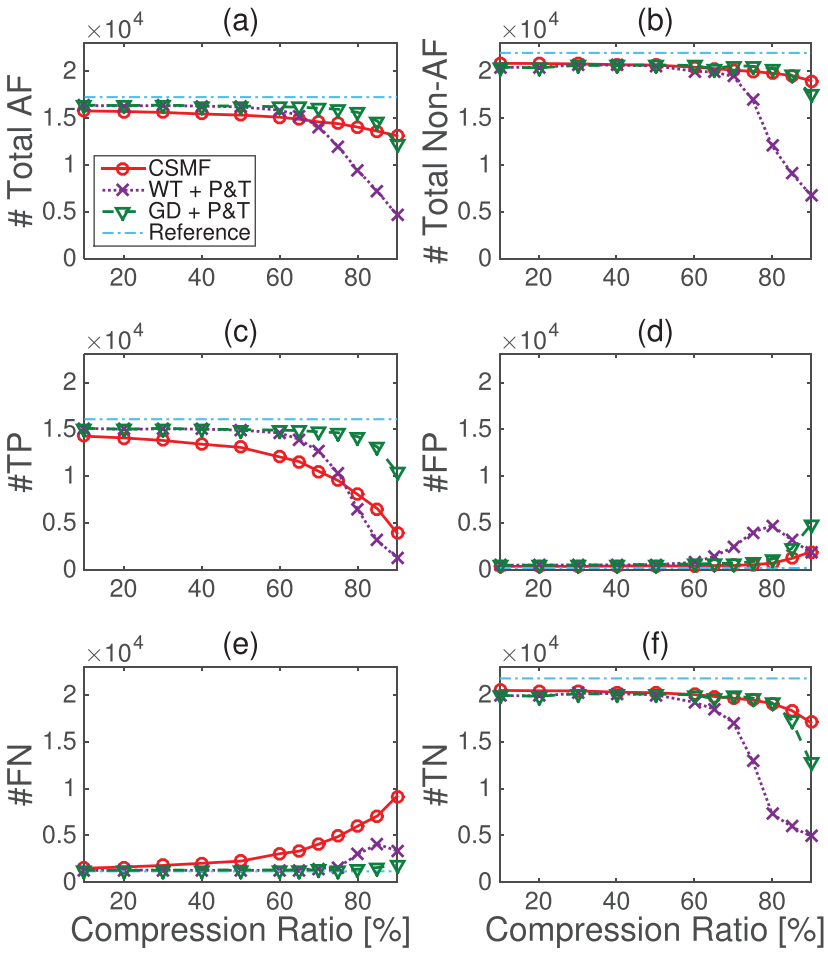

Figure 6. Total number of (a) AF episodes ($TP + FN$), (b) non-AF episodes ($TN + FP$). Number of (c) true positive (TP), (d) false positive (FP), (e) false negative (FN) and (f) true negative (TN) detections for the SVM AF classifier operating on QRS detected using CSMF or P&T detection after reconstruction using wavelet transform (WT) and Gaussian dictionary (GD). The reference numbers (dash-dot line) refer to the AF episodes and non-AF episodes found from the reference QRS.

ECG signals using the wavelet basis results in $\mathrm{Se}_{\mathrm{QRS}} = 97.01\%$ and $+\mathrm{P}_{\mathrm{QRS}} = 97.54\%$. The P&T method run on the reconstructed ECG signals using the Gaussian dictionary results in $\mathrm{Se}_{\mathrm{QRS}} = 96.98\%$ and $+\mathrm{P}_{\mathrm{QRS}} = 97.48\%$. These results are slightly higher than those obtained with P&T-based QRS detection on the raw ECG signals (see section 2.7.2), and can be explained by the filtering properties of the CS approach at low CR rates.

At CR levels higher than about 60–70%, the QRS detection accuracy of all three CS approaches declines rapidly. It is worth noting the difference between the wavelet basis recovery and Gaussian dictionary recovery. Figure 2(d) clearly shows that recovery performed using the wavelet basis leads to many missed QRS detections at high CR levels. Thus, as we can see in figures 3 and 4, detection on signals reconstructed using the wavelet basis has

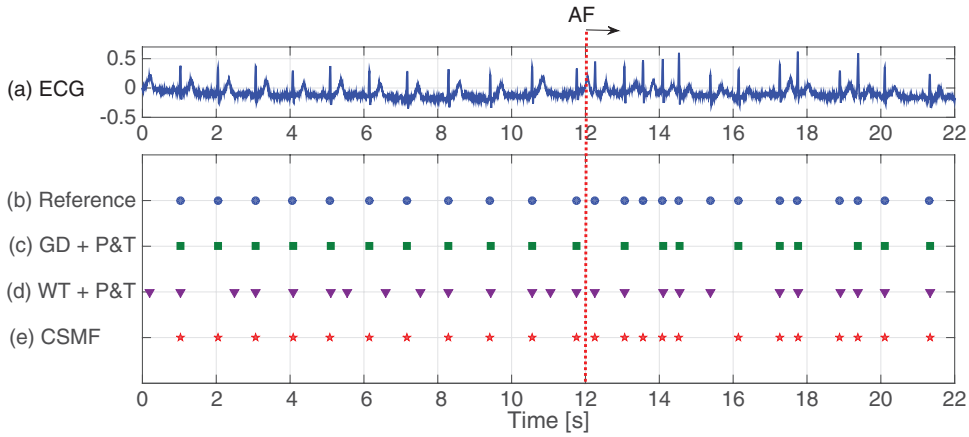

Figure 7. From top to bottom: (a) ECG signal (04746) at time 1:13:10 and (b) corresponding RR series of a non AF and AF episodes from the annotations file. The RR series detected after signal reconstruction using (c) Gaussian dictionary (GD) and (d) wavelet transform (WT). (e) RR series from the compressed beat detector (CSMF).

lower sensitivity and positive predictivity values than on signals recovered using the Gaussian dictionary. Indeed, the reconstruction process using the wavelet basis typically introduces artifacts that lead to incorrect QRS detections.

At the same CR level, the reconstructed ECG signals using the Gaussian dictionary, based on a model of QRS waveforms, exhibit less artifacts, leading to better accuracy for QRS detection. This can be seen in figure 5, which shows an example from record 05121. In particular, figure 5(a) shows the raw ECG signal and the corresponding annotated QRS complexes marked with triangles. Figures 5(b) and (c) depict the reconstructed ECG signals using the Gaussian dictionary and the wavelet basis, respectively, at CR = 75%. Triangles in (b) and (c) represent the detected QRS using the P&T method on the reconstructed signals. It can be seen that the artifacts present in the reconstructed ECG signal using the wavelet basis cause wrong beat detection. Obviously, if one or more QRS complexes are missed or wrongly detected, the resulting RR interval series and consequently AF classification performance, are compromised. In addition, for high CR levels, the proposed CSMF method gives higher sensitivity, but lower positive predictivity for QRS detection, than the method based on the wavelet basis. We note that reconstruction using the Gaussian dictionary gives the best results. We will analyze the complexity of the proposed approaches in section 3.3.

3.2. AF detection performance

As mentioned, the detector operates on segments of 30 consecutive beats within the manually annotated AF and non-AF time intervals. The reference total number of AF segments is given by the number of segments belonging to AF time intervals and obtained from the annotated QRS complexes. The reference total number of non-AF segments is computed similarly. It is important to note that, due to compression and errors in QRS detection, the total number of segments in AF time intervals for a given technique, computed as the sum of *TP* and *FN* classification decisions, is in general different from the reference value. The same happens for non-AF segments, defined as the sum of *TN* and *FP* after classification. Of course, if many QRS complexes are missed, we expect a large difference with respect to the reference values.

Table 2. Results of the performance metrics on uncompressed and compressed ECG signals using different reconstruction/detection methods.

Metric		CS reconstruction	QRS detector	Compression ratio												
				0%	10%	20%	30%	40%	50%	60%	65%	70%	75%	80%	85%	90%
Se (%)	Reference QRS	—	—	93.22	—	—	—	—	—	—	—	—	—	—	—	—
	Raw signals	—	P&T	92.97	—	—	—	—	—	—	—	—	—	—	—	—
	CS ECG signals	SL0 & WT	P&T	—	92.35	91.97	92.11	92.21	92.06	92.16	91.29	89.52	86.39	68.09	43.38	27.41
	CS ECG signals	SL0 & GD	P&T	—	92.15	91.35	92.10	92.02	91.91	91.93	91.90	91.67	91.75	91.02	89.25	84.83
	CS ECG signals	No	CSMF	—	90.47	89.63	88.47	86.85	85.24	79.79	77.63	72.00	66.01	57.10	47.87	29.88
Sp (%)	Reference QRS	—	—	99.14	—	—	—	—	—	—	—	—	—	—	—	—
	Raw signals	—	P&T	97.68	—	—	—	—	—	—	—	—	—	—	—	—
	CS ECG signals	SL0 & WT	P&T	—	97.61	97.54	97.59	97.49	97.36	96.08	92.91	87.65	76.50	60.94	65.04	72.65
	CS ECG signals	SL0 & GD	P&T	—	97.64	97.38	97.59	97.47	97.21	97.04	96.76	96.61	95.83	94.41	88.50	72.66
	CS ECG signals	No	CSMF	—	98.30	98.19	98.33	98.06	97.97	98.10	97.80	97.74	97.34	96.46	93.89	89.88
Acc (%)	Reference QRS	—	—	96.53	—	—	—	—	—	—	—	—	—	—	—	—
	Raw signals	—	P&T	95.28	—	—	—	—	—	—	—	—	—	—	—	—
	CS ECG signals	SL0 & WT	P&T	—	95.27	95.07	95.17	95.17	95.02	94.35	92.20	88.44	80.58	64.07	55.49	54.29
	CS ECG signals	SL0 & GD	P&T	—	95.20	94.72	95.16	95.06	94.88	94.79	94.60	94.45	94.05	92.93	88.82	77.66

	CS ECG signals	No	CSMF	—	94.93	94.51	94.10	93.27	92.55	90.32	89.27	86.92	84.22	80.13	75.01	65.37
PPV (%)	Reference QRS	—	—	98.83	—	—	—	—	—	—	—	—	—	—	—	—
	Raw signals	—	P&T	96.96	—	—	—	—	—	—	—	—	—	—	—	—
	CS ECG signals	SL0 & WT	P&T	—	96.87	96.77	96.79	96.67	96.48	94.91	90.79	84.00	72.09	57.63	49.44	40.63
	CS ECG signals	SL0 & GD	P&T	—	96.90	96.49	96.81	96.64	96.29	96.07	95.77	95.47	94.47	92.60	85.32	68.43
	CS ECG signals	No	CSMF	—	97.57	97.39	97.55	97.09	96.89	96.87	96.27	95.86	94.71	91.97	84.50	67.10
NPV (%)	Reference QRS	—	—	94.91	—	—	—	—	—	—	—	—	—	—	—	—
	Raw signals	—	P&T	94.04	—	—	—	—	—	—	—	—	—	—	—	—
	CS ECG signals	SL0 & WT	P&T	—	94.10	93.83	94.00	94.08	93.97	93.93	93.30	92.03	88.89	70.99	59.31	59.44
	CS ECG signals	SL0 & GD	P&T	—	93.95	93.44	93.95	93.92	93.85	93.87	93.73	93.70	93.73	93.19	91.66	87.27
	CS ECG signals	No	CSMF	—	93.17	92.62	91.91	90.91	89.95	86.79	85.64	82.80	79.90	76.03	72.13	64.98
J (%)	Reference QRS	—	—	92.36	—	—	—	—	—	—	—	—	—	—	—	—
	Raw signals	—	P&T	89.95	—	—	—	—	—	—	—	—	—	—	—	—
	CS ECG signals	SL0 & WT	P&T	—	89.96	89.51	89.70	89.71	89.42	88.24	84.20	77.17	62.89	29.03	8.42	0.06
	CS ECG signals	SL0 & GD	P&T	—	89.79	88.73	89.68	89.49	89.13	88.98	88.66	88.28	87.58	85.43	77.74	57.49
	CS ECG signals	No	CSMF	—	88.77	87.82	86.80	84.91	83.21	77.89	75.43	69.74	63.36	53.56	41.76	19.76

As a reference for the performance of AF detection in compressed/reconstructed signals, we perform classification based on the reference QRS positions provided in the dataset or detected by P&T on the raw original ECG signals. In these cases we obtain an accuracy Acc = 96.53% on provided QRS annotations and 95.28% using QRS detected with the P&T detector.

Figures 6(a) and (b) compare the total number of AF and non-AF segments for a given technique with the reference values. It can be seen that reconstruction with the wavelet basis exhibits a significant drop at compression ratios higher than 60%. This is consistent with figure 2, where it can be seen that at high CR, the method based on signal recovery using WT missed many QRS complexes, whereas the GD and the CSMF methods could detect almost as many beats as given by the reference annotated QRS complexes.

Figures 6(c)–(f) show *TP*, *FN*, *FP* and *TN* values for AF detection as a function of CR, for the three CS scenarios considered in this study.

The number of correctly classified AF segments, represented by the *TP* value, is reported in figure 6(c). It can be seen that *TP* starts to rapidly drop at CR >60% when AF detection is performed after reconstruction with the wavelet basis. Instead, when reconstruction is performed using the Gaussian dictionary, *TP* starts to significantly decrease at CR > 75%. The CSMF technique, applied directly in the compressed domain, results in a relatively small performance loss up to CR = 50% with a rapid decline at higher compression.

Figures 6(d)–(f) similarly show that for CR up to 60% the techniques have similar performance, while the WT and CSMF techniques degrade at higher compression. The method based on reconstruction with the Gaussian dictionary exhibits very good performance for CR up to about 75%. Note that the SVM detector tends to classify a segment with an RR pattern not consistent with AF as a non-AF segment, which is a safe harbour approach. Indeed, if a patient needs treatment, many AF segments would be present, and it is likely that eventually a positive trigger would be seen. This explains the larger FN values at high compression ratios.

An example of detected QRS complexes by the three CS techniques for non-AF and AF episodes is reported in figure 7. The figure shows a sample of record 04746, and, in particular, the AF episode occurs at time 1:13:10. The detected RR series after compression (CR = 80%) and reconstruction shows that WT leads to inaccurate QRS locations. In this example, the use of the Gaussian dictionary enables a better QRS detection that allows to correctly classify the normal rhythm and the AF episode. This also applies for CSMF detection on the CS measurements.

Table 2 summarizes the results for the SVM-based AF detector on the MIT-BIH atrial fibrillation database in a variety of scenarios, as described in section 2. In particular, the second columns specifies the technique used for the evaluation. 'Reference QRS' refers to the application of the SVM-based AF detector on annotated QRS complexes, while 'Raw signals' refers to classification after QRS detection using the P&T procedure on uncompressed signals, as specified in the fourth column. It is clear that the corresponding performance values help to quantify the performance of the CS-based techniques. Note that the CSMF method does not require signal reconstruction, as specified in the third column, where the reconstruction technique is indicated.

It can be seen from table 2 that the application of the AF detector on annotated QRS complexes ('Reference QRS') results in a very high Sp value equal to 99.14% and a relative low Se value equal to 93.22%. As mentioned before, this can be justified by the fact that the classifier tends to mark as non-AF those segments which do not exhibit a typical AF pattern. As expected, classification after QRS detection by employing the P&T algorithm on the uncompressed ECG signals also results in a high Sp of 97.68% and a relative low Se of 92.97%.

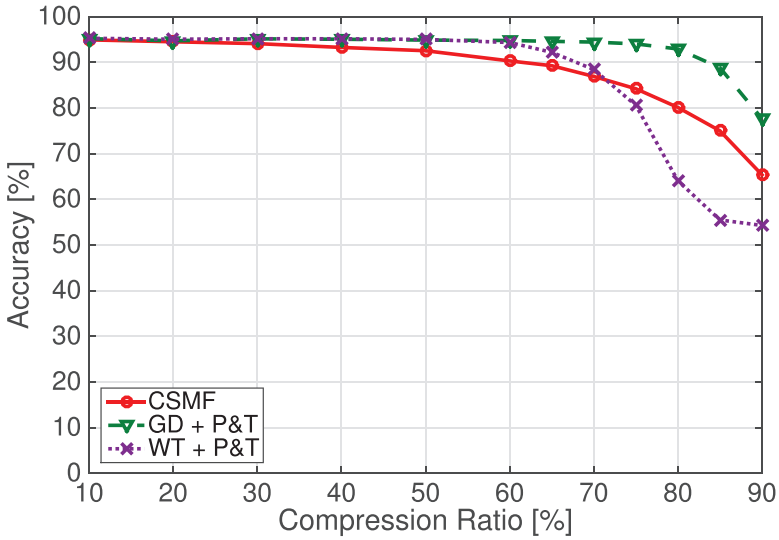

Figure 8. Output AF accuracy versus CR.

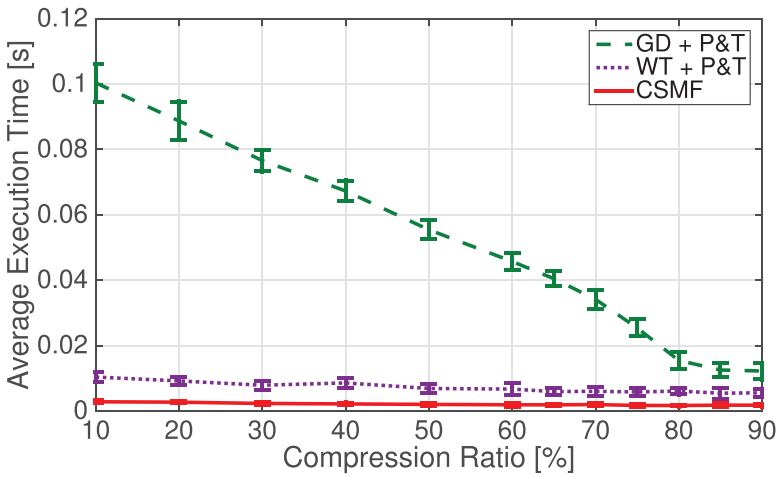

Figure 9. Average time required to process 1 s of signal. The error bar gives the standard deviation over multiple runs. For the CSMF the time is related to the QRS detection and for the other two methods the execution time includes both the time require to reconstruct the signal and perform the QRS detection using the P&T approach.

An overall picture of the accuracy of AF detection performance as a function of CR is given in figure 8. It can be seen from the figure and from table 2 that, for CR values up to about 50%, the AF detector applied to QRS complexes derived from the compressed signals, using the CS techniques described in this work, gives results comparable to those achieved when employing a standard QRS detector on the raw uncompressed signals. At a compression ratio equal to 60%, we have less than 1% loss for the WT and GD based techniques, and about a 5% loss for CSMF. At a compression ratio equal to 75%. the GD method guarantees a small performance loss of about 1.2%.

3.3. Execution time

In order to quantify the possible benefits of the new CSMF method against the methods based on CS reconstruction followed by P&T QRS detection, we compare the time required by the different schemes to process 1 s long ECG signal. For the CSMF method, the processing time is merely the time required for QRS detection on the compressed measurements, via matched filter computation in the compressed domain. In the other cases, the total time required by the CS reconstruction procedure followed by P&T QRS detection is taken into account. Results are reported in figure 9. Time measurement is based on implementation using MATLAB (R2016b) on a desktop computer with Intel(R) Core (TM) 2 Duo CPU 7400 @ 2.80 GHz, and 4GB of RAM.

The CSMF outperformed the other two methods in terms of execution time. Indeed, to process 1 s ECG signal, the CSFM takes 0.0028 s at CR $= 20\%$, and 0.0018 s for CR $= 90\%$. This means that to process a 1 hour long signal, the CSMF method only takes 10 s at CR $= 20\%$.

For the other two CS techniques that require reconstruction and P&T detection, the execution time at CR $= 20\%$ increases to 0.01 s and 0.1 s for the WT and GD methods, respectively. For CR $= 90\%$ the execution time becomes 0.0055 s and 0.01 s for the WT and GD methods, respectively. Thus, to process a 1 h long ECG signal at CR $= 20\%$, the total time required is about 36 s with the WT method and it further increases to about 6 minutes using the GD method. Moreover, it should be noted that QRS detection with the P&T method is applied after reconstruction of the whole signal, while the CSMF is applied to 1.5 s sliding windows, which allows real-time processing with a small delay.

4. Discussion

To detect AF automatically and reliably is a challenging task even on raw uncompressed ECG data. In our study, we investigated the effect of CS-based ECG compression on the accuracy of an AF detector applied to the processed data, for a wide range of compression ratios between 10% and 90%. To this end, two different sparsifying representations, in combination with the SL0 algorithm, were used to reconstruct the ECG signals from the CS measurements. Afterwards, the P&T algorithm was employed for QRS detection. Furthermore, we also describe a newly introduced beat detector that allows direct processing of the compressed measurements, without any signal reconstruction. Finally, the RR interval series obtained from the three different CS scenarios at different CR levels was used to perform AF detection using a previously reported state-of-the-art SVM-based model.

All three CS scenarios, i.e. reconstruction with the wavelet basis or the Gaussian dictionary followed by a standard (P&T detector, and the direct detection on compressed measurements (CSMF), exhibit similar characteristics for what concerns the AF classification quality metrics. In particular, at low CR levels, the AF detection results are comparable with those obtained on raw uncompressed ECG signals. However, for high CR values, the AF detection accuracy for the three methods decreases, as can be seen in figure 8. The results reveal that AF detection based on the new CSMF method has an acceptable performance loss, with respect to the techniques that require signal reconstruction, up to compression ratios of about 60%. This technique performs better than the WT-based method for CR higher than 70%. Indeed, CSMF reaches an accuracy equal to 92.55% at a 50% compression ratio, while at CR $= 90\%$, its accuracy decreases to 65.37%. AF detection after reconstruction using WT allows slightly better results up to CR$= 70\%$. However, its performance rapidly decreases at higher CR levels

and reaches an accuracy equal to 54.29% at CR = 90%. The best performance is achieved by the method with signal reconstruction using the Gaussian dictionary, which allows to reach accuracies 94.05% and 77.66% at CR = 75% and CR = 90%, respectively.

This study also highlights some drawbacks related to each of the three CS scenarios. One major drawback of the CSMF method is the quickly increasing number of false negative AF detections *FN* when CR> 50%. This is due to the SVM-detector tendency to favour non-AF classifications. The WT method has a reconstruction quality that decreases rapidly at high compression ratios, thus compromising classification quality. Overall, it appears that using the Gaussian dictionary for signal reconstruction enables a good AF detection up to a CR level of 75–80%, at the expense of increased reconstruction complexity.

The *democracy* property of compressive sensing consists in the fact that each measurement carries the same amount of information. Thus, the reconstruction quality depends only on how many measurements are received and not on the particular received subset. This allows to modulate the compression ratio by simply discarding or retaining some measurements. Considering the trade-off between AF classification accuracy, execution time, and compression, one could envision a two-stage processing system where the CSMF method is employed in the sensor for mild compression ratios up to CR = 60%. The system then switches to a higher compression, when transmission or recording is needed after AF episodes are detected, in view of reconstruction with GD followed by P&T detection. The switch simply consists in transmitting or recording fewer measurements. In a concrete scheme, one could acquire a compressed version of the signal using the analog CS implementation (Gangopadhyay *et al* 2014, Bellasi and Benini 2015) with a low CR, e.g. 50%, and use CSMF for AF detection. Then, the CR can be increased (up to 80%) by keeping a subset of the measurements in order to save/transmit a lower amount of data, still allowing accurate AF classification when the reconstruction is performed using the GD method.

As one could expect, there is a relationship between the AF detection accuracy and QRS detection accuracy. In particular Se_{QRS} starts to rapidly decline for CR > 60%, similarly to what happens for the AF detection accuracy, when reconstruction using the WT and CSMF methods are used. Furthermore, reconstruction using the Gaussian dictionary allows to obtain similar results at a higher CR = 75%.

Many studies related to CS-based ECG compression limited their assessment to the reconstruction quality, without evaluating the actual impact that signal reconstruction has on preserving relevant clinical information. In this study, we show that CS can be successfully employed as a compression technique for ECG signals when the final goal is to perform AF detection. As for reconstruction quality, we also show that the reliability of detected QRS complexes significantly depends on the sparsifying basis adopted for reconstruction.

5. Conclusions

The results of this study show that AF classification performed after CS-based compression allows us to correctly detect AF episodes when the compression ratio is lower than 60% or 75%, depending on the reconstruction/detection method adopted. In particular, we found that acceptable results are obtained for compression ratios up to 60% when AF classification is performed on signal reconstructed using wavelets as the sparsifying basis, or when the CSMF method is used. However, when a specifically designed sparsifying dictionary is used during signal reconstruction, good results are obtained for CR values as high as 75%. These findings

have positive implications concerning the acquisition and compression of ECG signals for clinical purposes using low-power wearable devices. Moreover, the possibility to correctly identify an AF episode directly on the compressed measurements represents a good opportunity for future long-term monitoring applications that need to process the data on energy-constrained devices.

ORCID

Giulia Da Poian https://orcid.org/0000-0002-8960-1077
Chengyu Liu https://orcid.org/0000-0003-1965-3020

References

Alemdar H and Ersoy C 2010 Wireless sensor networks for healthcare: a survey *Comput. Netw.* **54** 2688–710

Association for the Advancement of Medical Instrumentation 1994 American National Standard for Ambulatory Electrocardiographs, publication ANSI/AAMIEC38

Baraniuk R G 2007 Compressive sensing *IEEE Signal Process. Mag.* **24** 118–21

Bellasi D E and Benini L 2015 Energy-efficiency analysis of analog and digital compressive sensing in wireless sensors *IEEE Trans. Circuits Syst.* I **62** 2718–29

Camm A J *et al* 2010 Guidelines for the management of atrial fibrillation: the task force for the management of atrial fibrillation of the European Society of Cardiology (ESC) *Eur. Heart J.* **31** 2369–429

Candès E J 2008 The restricted isometry property and its implications for compressed sensing *C. R. Math.* **346** 589–92

Candès E J, Romberg J and Tao T 2006a Robust uncertainty principles: exact signal reconstruction from highly incomplete frequency information *IEEE Trans. Inf. Theory* **52** 489–509

Carrara M, Carozzi L, Moss T J, de Pasquale M, Cerutti S, Ferrario M, Lake D E and Moorman J R 2015 Heart rate dynamics distinguish among atrial fibrillation, normal sinus rhythm and sinus rhythm with frequent ectopy *Physiol. Meas.* **36** 1873

Da Poian G, Bernardini R and Rinaldo R 2014 Gaussian dictionary for compressive sensing of the ECG signal *Proc. IEEE Workshop on Biometric Measurements and Systems for Security and Medical Applications* (IEEE) pp 80–5

Da Poian G, Bernardini R, Rinaldo R and Clifford G D 2017 Matched filtering for heart rate estimation on compressive sensing ECG measurements *IEEE Trans. Biomed. Eng.* submitted

Donoho D L 2006 Compressed sensing *IEEE Trans. Inf. Theory* **52** 1289–306

Gangopadhyay D, Allstot E G, Dixon A M, Natarajan K, Gupta S and Allstot D J 2014 Compressed sensing analog front-end for bio-sensor applications *IEEE J. Solid State Circuits* **49** 426–38

Goldberger A L, Amaral L A, Glass L, Hausdorff J M, Ivanov P C, Mark R G, Mietus J E, Moody G B, Peng C K and Stanley H E 2000 Physiobank, physiotoolkit, and physionet components of a new research resource for complex physiologic signals *Circulation* **101** e215–20

Hamilton P S and Tompkins W J 1986 Quantitative investigation of QRS detection rules using the MIT/BIH arrhythmia database *IEEE Trans. Biomed. Eng.* **12** 1157–65

Kaplan D T 1990 Simultaneous QRS detection and feature extraction using simple matched filter basis functions *Computers Cardiology, Proc.* (IEEE) pp 503–6

Ko J, Lu C, Srivastava M B, Stankovic J A, Terzis A and Welsh M 2010 Wireless sensor networks for healthcare *Proc. IEEE* **98** 1947–60

Kohler B-U, Hennig C and Orglmeister R 2002 The principles of software QRS detection *IEEE Eng. Med. Biol. Mag.* **21** 42–57

Li Q, Liu C, Oster J and Clifford G D 2016 Signal processing and feature selection preprocessing for classification in noisy healthcare data *Machine Learning for Healthcare Technologies* ch 3, pp 33–58

Lip G Y H *et al* 2016 Atrial fibrillation *Nat. Rev. Disease Primers* **2** 16016

Liu C, Li K, Zhao L, Liu F, Zheng D, Liu C and Liu S 2013 Analysis of heart rate variability using fuzzy measure entropy *Comput. Biol. Med.* **43** 100–8

Mamaghanian H, Khaled N, Atienza D and Vandergheynst P 2011 Compressed sensing for real-time energy-efficient ECG compression on wireless body sensor nodes *IEEE Trans. Biomed. Eng.* **58** 2456–66

Mohimani H, Babaie-Zadeh M and Jutten C 2009 A fast approach for overcomplete sparse decomposition based on smoothed norm *IEEE Trans. Signal Process.* **57** 289–301

Pan J and Tompkins W J 1985 A real-time QRS detection algorithm *IEEE Trans. Biomed. Eng.* **32** 230–6

Pinheiro E C, Postolache O A and Girao P S 2010a Implementation of compressed sensing in telecardiology sensor networks *Int. J. Telemed. Appl.* **2010** 7

Ruha A, Sallinen S and Nissila S 1997 A real-time microprocessor QRS detector system with a 1 ms timing accuracy for the measurement of ambulatory HRV *IEEE Trans. Biomed. Eng.* **44** 159–67

Tateno K and Glass L 2000 A method for detection of atrial fibrillation using RR intervals *Computers in Cardiology* (IEEE) pp 391–4